

Paramagnetic Defect Centers at the MgO Surface. An Alternative Model to Oxygen Vacancies

Davide Ricci,[†] Cristiana Di Valentin,[†] Gianfranco Pacchioni,^{*,†} Peter V. Sushko,[‡] Alexander L. Shluger,[‡] and Elio Giamello[§]

Contribution from the Dipartimento di Scienza dei Materiali, Università di Milano-Bicocca, Istituto Nazionale per la Fisica della Materia, Via R. Cozzi, 53 - 20125, Milano, Italy, Department of Physics and Astronomy, University College London, Gower Street, London WC1E 6BT, U.K., Dipartimento di Chimica IFM, Università di Torino, and Istituto Nazionale per la Fisica della Materia, via P. Giuria 5, I-10125 Torino, Italy

Received August 21, 2002; E-mail: gianfranco.pacchioni@unimib.it

Abstract: On the basis of embedded cluster calculations, we propose a new model for the structure of paramagnetic color centers at the MgO surface usually denoted as $F_S(H)^+$ (an electron trapped near an adsorbed proton). These centers are produced by exposing the surface of polycrystalline MgO to H_2 followed by UV irradiation. We demonstrate that properties of H atom adsorbed at surface sites such as step edges (MgO_{step}) and reverse corner sites (MgO_{RC}), formed at the intersection of two step edges, are compatible with a number of features observed for $F_S(H)^+$. Our calculations suggest that (i) H_2 dissociates at the reverse corner site heterolytically and that there is no barrier for this exothermic reaction; (ii) the calculated vibrations of the resulting $MgO_{RC}(H^+)(H^-)$ complex are fully consistent with the measured ones; (iii) desorption of a neutral H atom from the diamagnetic precursor requires UV light and leads to the formation of stable neutral paramagnetic centers at the surface, $MgO_{step}(H^+)(e^-)_{trapped}$ and $MgO_{RC}(H^+)(e^-)_{trapped}$. The computed isotropic hyperfine coupling constants and optical transitions of these centers are in broad agreement with the existing experimental data. We argue that these centers, which do not belong to the class of "oxygen vacancies", are two of the many possible forms of the $F_S(H)^+$ defect center.

1. Introduction

The chemical activity of oxide surfaces is closely related to the number and nature of surface defects created during material synthesis.¹ The exact nature of these defects, however, is difficult to establish because usually they represent a minority of the surface sites, which in turn are only a small fraction of the total number of atoms in the material. For this reason, theoretical calculations of defect models and their spectroscopic and thermodynamic properties are crucial for the identification of the chemical nature of defects at oxide surfaces.^{2,3} Substantial progress has been made in recent years in applications of this combined experimental-theoretical approach to the study of surface defects and surface morphology of magnesium oxide, MgO.² MgO has important applications in catalysis and as a substrate for growing various materials.⁴ It has been the focus of fundamental research for many years as a prototype ionic

oxide with a relatively well-defined surface structure. Still, models of many surface defects are not established.

Trapped electrons represent a special class of such defects at the MgO surface. These defects were first investigated in the bulk of the material where they give rise to typical optical and electron paramagnetic resonance (EPR) spectra.^{1,5} Two types of F centers exist in the bulk of bivalent oxides, such as MgO and CaO: one containing two electrons in the oxygen vacancy, called an F center, and the other, containing only one electron, known as an F^+ center.⁶ The optical absorption associated with these centers determines the color of the sample (and the name of the centers, from Farbe, the German word for color).⁶ Because paramagnetic F^+ centers can be studied by EPR, they are better characterized than neutral F centers. The model of a bulk F center in MgO has been extended to the surface by Tench,^{7,8} who proposed the existence of anion vacancies on the terraces of MgO (or F_S centers). More recently, Giamello and co-workers^{9,10} have revisited the problem of surface trapped electrons proposing new types of centers still based on the presence of surface oxygen vacancies but introducing the idea

[†] Università di Milano-Bicocca.

[‡] University College London.

[§] Università di Torino.

* Address correspondence to this author.

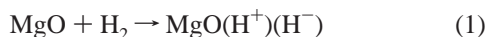
- (1) Tilley, R. J. D. *Principles and Applications of Chemical Defects*; Stanley Thornes: Cheltenham, 1998.
- (2) Pacchioni, G. In *The Chemical Physics of Solid Surfaces – Oxide Surfaces*; Woodruff, P., Ed.; Elsevier: Amsterdam, 2000; Vol. 9, pp 94–135.
- (3) Pacchioni, G. *Surf. Rev. Lett.* **2000**, *7*, 277.
- (4) *Chemisorption and Reactivity of Supported Clusters and Thin Films*; Lambert, R. M., Pacchioni, G., Eds.; Kluwer: Dordrecht, 1997; NATO ASI Series E, Vol. 331.

- (5) Wertz, J. E.; Auzins, P.; Weeks, R. A.; Silsbee, R. H. *Phys. Rev.* **1957**, *107*, 1535.
- (6) Kappers, L. A.; Kroes, R. L.; Hensley, E. B. *Phys. Rev. B* **1970**, *10*, 4151.
- (7) Tench, A. J.; Nelson, R. L. *J. Colloid Interface Sci.* **1968**, *26*, 364.
- (8) Tench, A. J. *Surf. Sci.* **1971**, *25*, 625.
- (9) Giamello, E.; Paganini, M. C.; Murphy, D.; Ferrari, A. M.; Pacchioni, G. *J. Phys. Chem.* **1997**, *101*, 971.
- (10) Paganini, M. C.; Chiesa, M.; Giamello, E.; Coluccia, S.; Martra, G.; Murphy, D. M.; Pacchioni, G. *Surf. Sci.* **1999**, *421*, 246.

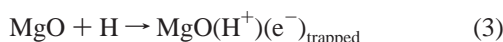
that the latter ones are localized in particular regions of the crystals (edges, steps, corners) where the ion coordination is lower than at the terraces. The localization of these centers on the surface is proved by the instantaneous reaction with adsorbed gases which form radical anions with complete quenching of the preexisting electron traps.^{11,12}

Although several experimental and theoretical studies point to the existence of surface F_S centers,^{13–24} their exact nature has not yet been unambiguously identified. The natural abundance of these centers (or at least of trapped electrons) in high-surface area MgO samples prepared, for instance, by thermal decomposition of $Mg(OH)_2$ is too low to be monitored by UV–vis spectroscopy and even by the highly sensitive EPR technique. However, the number of populated centers can be significantly increased using various chemical or photochemical treatments. One way of achieving that is to deposit low dosage of alkali metals on the surface.^{25–27} On defect-rich surfaces, the alkali atoms lose their valence electron, and positive metal ions are adsorbed at oxygen sites; the electrons are thought to be trapped at preexisting bare oxygen vacancies, F_S^{2+} centers, and give rise to the typical signal of F_S^+ centers. The second approach is based on the adsorption of molecular hydrogen, which dissociates at specific sites into H^+ (stabilized at surface O^{2-} anions) and H^- species (stabilized at surface Mg^{2+} cations).⁸ Under UV irradiation, the H^- species transform into $H + e^-$, where the electron is trapped at the surface, producing an EPR-active center known as $F_S(H)^+$.⁹

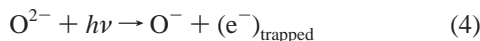
The whole reaction is therefore



The H atom produced in step 2 can further react with another MgO site and form another $F_S(H)^+$ center:



Another reaction channel, leading to the electron trapping under irradiation in H_2 atmosphere, is due to the reaction of molecular hydrogen with surface O^- ions formed by the UV irradiation at low coordinated surface sites:²⁸



Reaction 5 produces atomic hydrogen, which can react according to reaction 3 with an acceptor site to form trapped electrons. The neutral H species are thought to be mobile on the surface terrace, and therefore the site for electron trapping according to reaction 3 could be at a remote location from the site of H_2 dissociation. It is important to note that EPR spectra of F_S^+ centers consistently show a coupling of the electron spin with the nuclear spin of the 1H nuclide.⁹ Therefore, trapped electrons in reactions 2 and 3 must reside near an adsorbed proton in the form of an OH group on the surface. This is why the center has been named $F_S(H)^+$.⁹ Most of the EPR data on trapped electrons at the surface of MgO reported so far refer to the $F_S(H)^+$ center; unambiguous measurements of the EPR properties of a bare F_S^+ center, without proton, do not seem to exist.

Bare surface anion vacancies, F_S^{2+} centers, have long been considered as a natural choice for a preexisting site which traps an electron and becomes a paramagnetic F_S^+ center. However, the F_S^{2+} centers are diamagnetic and do not have specific optical absorption features. Therefore, the presence and concentration of F_S^{2+} centers are very difficult to verify experimentally. Moreover, the theoretical calculations indicate that the formation energy of charged F_S^{2+} centers, which result formally from the removal of an O^{2-} ion from the surface, is very high,^{20,13} suggesting that their number at thermal equilibrium can be comparatively small. It has been suggested that these centers can be formed in the final steps of the process of dehydration at high temperatures^{9,10} and that only low-coordinated F_S^{2+} centers at corners and kinks can be involved in creation of $F_S(H)^+$ centers.¹⁰ The existence of at least two types of $F_S(H)^+$ centers²⁹ and of a wide variety of transient electron and hole traps at MgO surfaces³⁰ suggested that a wider approach to the problem of electron traps at this surface, not only focused on anion vacancies, can prove to be more fruitful.

Several trapping sites on the MgO surface not connected to the presence of doubly charged oxygen vacancies, F_S^{2+} , have been suggested recently.^{10,28–33} One of these is the double Mg and O vacancy, V_{MgO} .^{28–33} This neutral defect has much lower formation energy than the F_S^{2+} center and can trap one electron and transform into an EPR-active paramagnetic center.^{31,32} Even low-coordinated Mg^{2+} single ion sites, such as kinks and corners, can also serve as surface electron traps.^{33,34} However, all of these centers are “shallow traps”, where the electron is bound by 1–1.5 eV. These energies are large enough that the traps are thermally stable at room temperature, but they cannot explain the optical excitations in the visible region characteristic of the color centers formed at the MgO surface.¹⁰ These centers cannot easily account for the existence of what is usually called the $F_S(H)^+$ center, with an electron trapped near an adsorbed proton. To address this issue requires a more systematic

- (11) Pacchioni, G.; Ferrari, A. M.; Giamello, E. *Chem. Phys. Lett.* **1996**, *255*, 58.
 (12) Chiesa, M.; Giamello, E.; Paganini, M. C.; Pacchioni, G.; Soave, R.; Murphy, D. M.; Sojka, Z. *J. Phys. Chem.* **2001**, *105*, 497.
 (13) Scorza, E.; Birkenheuer, U.; Pisani, C. *J. Chem. Phys.* **1997**, *107*, 9645.
 (14) Sharma, R. R.; Stoneham, A. M. *J. Chem. Soc., Faraday Trans.* **1976**, *2*, 913.
 (15) Gibson, A.; Haydock, R.; LaFemina, J. P. *Phys. Rev.* **1994**, *50*, 2582.
 (16) Kantorovich, L. N.; Holender, J. M.; Gillan, M. J. *Surf. Sci.* **1995**, *343*, 221.
 (17) Castanier, E.; Noguera, C. *Surf. Sci.* **1996**, *364*, 1.
 (18) Finocchi, F.; Goniakowski, J.; Noguera, C. *Phys. Rev. B* **1999**, *59*, 5178.
 (19) Pisani, C.; Corà, F.; Dovesi, R.; Orlando, R. *J. Electron Spectrosc.* **1994**, *96*, 1.
 (20) Ferrari, A. M.; Pacchioni, G. *J. Phys. Chem.* **1995**, *99*, 17010.
 (21) Sushko, P. V.; Shluger, A. L.; Catlow, C. R. A. *Surf. Sci.* **2000**, *450*, 153.
 (22) Pacchioni, G.; Pescarmona, P. *Surf. Sci.* **1998**, *412/413*, 657.
 (23) Illas, F.; Pacchioni, G. *J. Chem. Phys.* **1998**, *108*, 7835.
 (24) Sousa, C.; Pacchioni, G.; Illas, F. *Surf. Sci.* **1999**, *429*, 217.
 (25) Giamello, E.; Ferrero, A.; Coluccia, S.; Zecchina, A. *J. Phys. Chem.* **1991**, *95*, 9385.

- (26) Giamello, E.; Murphy, D.; Ravera, L.; Coluccia, S.; Zecchina, A. *J. Chem. Soc., Faraday Trans.* **1994**, *90*, 3167.
 (27) Murphy, D.; Giamello, E. *J. Phys. Chem.* **1995**, *99*, 15172.
 (28) Sterrer, M.; Diwald, O.; Knoezinger, E. *J. Phys. Chem. B* **2000**, *104*, 3601.
 (29) Murphy, D. M.; Farley, R. D.; Purnell, I. J.; Rowlands, C.; Yacob, A. R.; Paganini, M. C.; Giamello, E. *J. Phys. Chem. B* **1999**, *103*, 1944.
 (30) Pinarello, G.; Pisani, C.; D'Ercole, A.; Chiesa, M.; Paganini, M. C.; Giamello, E.; Diwald, O. *Surf. Sci.* **2001**, *494*, 95.
 (31) Ojamäe, L.; Pisani, C. *J. Chem. Phys.* **1998**, *109*, 10984.
 (32) Ricci, D.; Pacchioni, G.; Sushko, P. V.; Shluger, A. L. *J. Chem. Phys.* **2002**, *117*, 2844.
 (33) Sushko, P. V.; Gavartin, J. L.; Shluger, A. L. *J. Phys. Chem. B* **2002**, *106*, 2269.
 (34) Sushko, P. V.; Shluger, A. L.; Baetzold, R. C.; Catlow, C. R. A. *J. Phys.: Condens. Matter* **2000**, *12*, 8257.

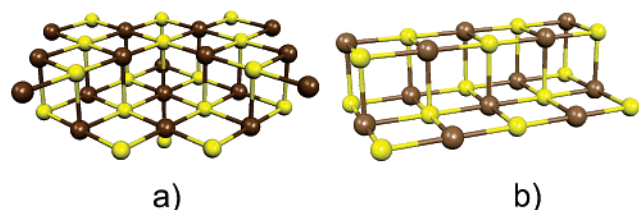


Figure 1. (a) $\text{Mg}_{17}\text{O}_{17}$ cluster model of a reverse corner site at the MgO surface, MgO_{RC} . (b) $\text{Mg}_{12}\text{O}_{13}$ cluster model of a step site at the MgO surface, MgO_{step} . The structures correspond to the quantum-mechanical (QM) part of region I in our embedded clusters. The remaining part of region I is represented by classical shell model ions. At the interface between QM and the shell model ions are 22 Mg^* atoms represented by effective core potentials. Region I is then embedded in about 3000 point charges (region II). Only the QM ions are shown for simplicity. Dark spheres, Mg; white spheres, O.

approach to the problem and modeling reactions 1–3 for some particular surface sites.

In this paper, we focus mainly on one particular surface site, the reverse corner, MgO_{RC} , Figure 1a, at the MgO surface and demonstrate that it can be responsible for reactions 1 and 2. We then demonstrate that decomposition of the H_2 molecule at MgO surface sites can lead to the formation of $\text{MgO}_{\text{RC}}(\text{H}^+)(\text{e}^-)_{\text{trapped}}$. The analysis is extended to a similar site at a step, $\text{MgO}_{\text{step}}(\text{H}^+)(\text{e}^-)_{\text{trapped}}$, Figure 1b. These are new models of electron traps, which may account for a number of experimental facts. We suggest that $\text{MgO}_{\text{RC}}(\text{H}^+)(\text{e}^-)_{\text{trapped}}$ and $\text{MgO}_{\text{step}}(\text{H}^+)(\text{e}^-)_{\text{trapped}}$ are two forms of the $\text{F}_s(\text{H})^+$ center observed in EPR experiments. These sites are representative of a whole family of similar sites existing at the MgO surface.

A brief summary of the computational scheme adopted for the calculations is given in section 2. Section 3a discusses the reverse corner as a shallow electron trap with the electron affinity of about 1 eV. In section 3b, we show that the H_2 molecule can heterolytically dissociate at the MgO_{RC} site with a barrier-less exothermic reaction and form the $\text{MgO}_{\text{RC}}(\text{H}^+)(\text{H}^-)$ complex. Vibrational properties of this complex are discussed in section 3c. In section 3d and 3e, the results of theoretical calculations of the stability and electronic and vibrational properties of the $\text{MgO}_{\text{RC}}(\text{H}^+)(\text{e}^-)_{\text{trapped}}$ center are presented. Similar results calculated for the $\text{MgO}_{\text{step}}(\text{H}^+)(\text{e}^-)_{\text{trapped}}$ center are presented in section 3f; in section 3g, we show that the process is specific to low-coordinated sites and does not occur on terraces. The conclusions are summarized in the last section. We also discuss some technical aspects of the description of these shallow traps in the Appendix.

2. Details of Calculations

To calculate the properties of the reverse corner site at the MgO surface, we employed an embedded cluster method (for details, see refs 21 and 33). The MgO crystal is represented by a large finite cluster, divided into regions I and II as briefly described below. Hemispherical region I is centered on a defect site and includes a quantum-mechanically treated cluster (QM cluster) surrounded by interface ions and classical shell model ions.^{21,34} The remaining part of the cluster, region II, is represented by classical nonpolarizable ions. All of the classical ions interact among themselves via interatomic potentials. The interface atoms interact quantum mechanically with atoms in the QM cluster and classically with other interface atoms and with classical atoms in regions I and II. The interaction between

the QM atoms and classical atoms in regions I and II is also included and is described using short-range classical potentials. All centers in region I are allowed to relax simultaneously during the geometry optimization. Ions in region II remain fixed and provide an accurate electrostatic potential (EP) within region I.

The interface between QM cluster and classical ions is needed to prevent an artificial spreading of electronic states outside of the QM cluster. The interface includes Mg^{2+} ions only (hereafter denoted as Mg^*); these are represented using a semilocal effective core pseudopotential (ECP),³⁵ which is a simplified version of a more rigorous potential proposed by Barandiaran and Seijo.³⁶ The use of all electron Mg^{2+} interface ions has also been considered, and the results are described in the Appendix.

This hybrid scheme is implemented in the GUESS code,²¹ which provides the shell model representation for the classically treated part of the system and an interface with the Gaussian 98 package³⁷ for ab initio calculations of the QM cluster. The GUESS code allows us to calculate forces acting on all centers in region I, both QM and classical (cores and shells), and simultaneously optimize their positions using the BFGS technique³⁸ for the energy minimization. The total energy and the electronic structure of the QM cluster are calculated by solving standard Kohn–Sham equations which include the matrix elements of the electrostatic potential due to all classical point charges in regions I and II computed on the basis functions of the cluster.

To model the reverse corner site, MgO_{RC} , Figure 1a, we used a cluster formed by $20 \times 20 \times 8$ atoms so that the surface terrace itself was modeled by a square of 20×20 atoms. From this terrace, a 5×5 ions fragment of the top layer has been removed to generate a model of two steps, which form a reverse corner at their intersection point. Similarly, one-half of the top layer was removed to model the (100) step, Figure 1b. In our calculations, we used stoichiometric or almost stoichiometric QM clusters so that the number of electrons assigned to them was uniquely defined (the use of nonstoichiometric clusters will be discussed in the Appendix). The reverse corner site and the step edge were modeled using $\text{Mg}_{17}\text{O}_{17}\text{Mg}^{*22}$ and $\text{Mg}_{12}\text{O}_{13}\text{Mg}^{*22}$, respectively, Figure 1.

The quantum-mechanical calculations were carried out using the density functional theory (DFT), where the gradient corrected Becke's three parameters hybrid exchange functional³⁹ in combination with the correlation functional of Lee, Yang, and Parr⁴⁰ (B3LYP) was employed. The parameters of the classical shell model potentials used in this work were optimized to

(35) Stevens, W.; Bach, H.; Krauss, J. *J. Chem. Phys.* **1984**, *81*, 6026.

(36) Barandiaran, Z.; Seijo, L. *J. Chem. Phys.* **1988**, *89*, 5739.

(37) Frisch, M. J.; Trucks, G. W.; Schlegel, H. B.; Scuseria, G. E.; Robb, M. A.; Cheeseman, J. R.; Zakrzewski, V. G.; Montgomery, J. A., Jr.; Stratmann, R. E.; Burant, J. C.; Dapprich, S.; Millam, J. M.; Daniels, A. D.; Kudin, K. N.; Strain, M. C.; Farkas, O.; Tomasi, J.; Barone, V.; Cossi, M.; Cammi, R.; Mennucci, B.; Pomelli, C.; Adamo, C.; Clifford, S.; Ochterski, J.; Petersson, G. A.; Ayala, P. Y.; Cui, Q.; Morokuma, K.; Malick, D. K.; Rabuck, A. D.; Raghavachari, K.; Foresman, J. B.; Cioslowski, J.; Ortiz, J. V.; Stefanov, B. B.; Liu, G.; Liashenko, A.; Piskorz, P.; Komaromi, I.; Gomperts, R.; Martin, R. L.; Fox, D. J.; Keith, T.; Al-Laham, M. A.; Peng, C. Y.; Nanayakkara, A.; Gonzalez, C.; Challacombe, M.; Gill, P. M. W.; Johnson, B. G.; Chen, W.; Wong, M. W.; Andres, J. L.; Head-Gordon, M.; Replogle, E. S.; Pople, J. A. *Gaussian 98*, revision A.6; Gaussian, Inc.: Pittsburgh, PA, 1998.

(38) Dennis, J. E.; Sabel, R. *Numerical Methods for Unconstrained Optimization and Nonlinear Equations*; Prentice-Hall: Englewood Cliffs, NJ, 1983.

(39) Becke, A. D. *J. Chem. Phys.* **1993**, *98*, 5648.

(40) Lee, C.; Yang, W.; Parr, R. G. *Phys. Rev. B* **1988**, *37*, 785.

reproduce properties of small MgO clusters calculated quantum mechanically.⁴¹

The standard 6-31G basis set for QM cluster Mg and O atoms was used in most calculations.^{42,43} The 6-311+G** basis⁴⁴ was used on the H atoms. No basis functions were set on the interface Mg* atoms. We have shown in previous studies that this procedure produces similar results to those obtained by placing floating functions at the site where the electron is supposed to be trapped.⁴⁵

The hyperfine interactions of the electron spin with the nuclear spin of the ²⁵Mg and ¹H nuclides have been determined for paramagnetic centers. The hyperfine spin-Hamiltonian, $H_{\text{hfc}} = \mathbf{S} \cdot \mathbf{A} \cdot \mathbf{I}$, is given in terms of the hyperfine matrix **A** which describes the coupling of the electron with the nuclear spin.⁴⁶ The components of **A** can be represented as the sum of an isotropic part, a_{iso} , related to the spin density on the nucleus, and a dipolar part, the matrix **B**. Here we concentrate on the isotropic part of the interaction, and we compare the computed values with those deduced from EPR spectra.

The excitation energies of the MgO_{RC}(H⁺)(e⁻)_{trapped} and MgO_{step}(H⁺)(e⁻)_{trapped} centers were computed using the time-dependent density functional approach (TD-DFT), a method which has recently opened new possibilities for the study of excited states in solids. For molecular systems, TD-DFT is known to provide a good accuracy.^{47–50} Some of us have successfully applied TD-DFT for the study of point defects in SiO₂.⁵¹

3. Results and Discussion

A. Electron Trapping at MgO_{RC} Defect Center. In this paper, we would like to build a model of an electron trap on the MgO(001) surface based solely on topographic surface features abundant at the surface. We have shown that corner oxygen vacancies and low-coordinated Mg sites can serve as electron traps.³³ In this section, we consider a reverse corner, MgO_{RC}, and demonstrate that it can serve as an electron trap too. We expect that sites such as this should be abundant at stepped surfaces, and unlike corners and kinks they have not been studied before.

The MgO_{RC} site was modeled using an Mg₁₇O₁₇Mg*₂₂ cluster, Figure 1a. The electronic affinity (EA) of the reverse corner site was calculated as the difference of total energies of the fully relaxed MgO_{RC} and MgO_{RC}(e⁻)_{trapped} centers and is 0.7 eV. This is similar to the EA found for other shallow traps at the MgO surface, such as divacancies³² or three-coordinated Mg ions.³³ It is important to mention that the vertical ionization potential

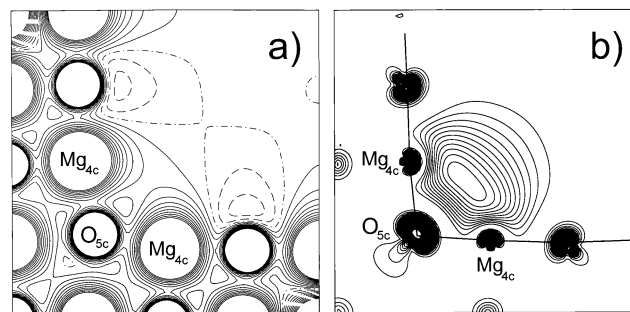


Figure 2. (a) Electrostatic potential of the MgO_{RC} center in the plane of the top layer obtained with the Mg₁₇O₁₇Mg*₂₂ cluster. Isocontour lines are plotted in intervals of 0.05 au. Solid, dashed, and dotted–dashed curves refer to positive, negative, and zero potential, respectively. (b) Spin density map of the MgO_{RC}(e⁻)_{trapped} center in the plane of the top layer obtained with the Mg₁₇O₁₇Mg*₂₂ cluster.

of the fully relaxed MgO_{RC}(e⁻)_{trapped} defect is considerably higher, 1.68 eV, thus confirming that electrons trapped at these sites are thermally stable. However, these sites cannot explain the color of the samples. The localization of the electron in the reverse corner is a consequence of the strong electrostatic potential at this site, Figure 2a. The spin density plots clearly show that the electron is confined in a region between the two four-coordinated Mg²⁺ ions, Figure 2b. This leads to a strong hyperfine interaction of the unpaired electron spin with these two ions: $a_{\text{iso}}(^{25}\text{Mg}) = 16$ G.

The calculation of the EA of a neutral cluster, that is, the calculation of the total energy of a cluster anion, is a delicate problem which requires accurate embedding procedures. The value of EA given above, 0.7 eV, can be affected by some uncertainties. The dependence of EA values on the computational method is discussed in the Appendix. However, while the absolute values of EA may depend on the treatment, the qualitative conclusion that MgO_{RC} is a shallow trap is not.

B. Modeling Interaction of H₂ with Reverse Corner. We have shown above that the MgO_{RC} site belongs to the family of shallow electron traps on the MgO surface. To further show that it can serve as a prototype F_S(H)⁺ center requires modeling the H₂ dissociation at this site and then demonstrating that an electron can be trapped at this site according to reaction 3. In this section, we provide firm evidence for this. To study the dissociation of H₂, reaction 1, at the reverse corner, the geometry optimization has been started by placing an H atom close to an oxygen anion at a step, O_{4c}, and the second H atom above the triangular face formed by three exposed Mg²⁺ cations, two of which are four-coordinated and one five-coordinated; see configuration 1 shown in Figure 3a. In a second calculation, one H atom has been placed above the five-coordinated O of the reverse corner; see configuration 2 shown in Figure 3b. In both cases, the optimization results in a formation of an OH group with a typical distance of 0.98 Å, with a second H atom being located at about 2.75 Å from the first H atom and 2.1 Å from the closest Mg cation. This corresponds to the heterolytic dissociation of H₂, as confirmed by the atomic charges; according to both Mulliken and natural population analyses, 0.5 electrons are associated to the H atom bound to the O²⁻ anion, while 1.8 electrons are associated to the other H. Thus, from now on we identify the two H atoms as the “proton”, H⁺, and the “hydride”, H⁻, respectively.

The H₂ dissociation is exothermic by 0.54 eV for complex 1 and by 0.22 eV for complex 2; experimentally, the average heat

- (41) Shluger, A. L.; Rohl, A. L.; Gay, D. H.; Williams, R. T. *J. Phys.: Condens. Matter* **1994**, *6*, 1825.
 (42) Francl, M. M.; Petro, W. J.; Hehre, W. J.; Binkley, J. S.; Gordon, M. S.; De Fries, D. J.; Pople, J. A. *J. Chem. Phys.* **1982**, *77*, 3654.
 (43) Hehre, W. J.; Ditchfield, R.; Pople, J. A. *J. Chem. Phys.* **1972**, *56*, 2257.
 (44) Krishnan, R.; Binkley, J. S.; Seeger, R.; Pople, J. A. *J. Chem. Phys.* **1980**, *72*, 650.
 (45) Ferrari, A. M.; Soave, R.; D’Ercolo, A.; Pisani, C.; Giannello, E.; Pacchioni, G. *Surf. Sci.* **2001**, *479*, 83.
 (46) Weil, J. A.; Bolton, J. R.; Wertz, J. E. *Electron Paramagnetic Resonance*; John Wiley & Sons: New York, 1994.
 (47) Casida, M. E. In *Recent Developments and Applications of Modern Density Functional Theory, Theoretical and Computational Chemistry*; Seminario, J. M., Ed.; Elsevier: Amsterdam, 1996; Vol. 4.
 (48) Casida, M. E.; Jamorki, C.; Casida, K. C.; Salahub, D. R. *J. Chem. Phys.* **1998**, *108*, 4439.
 (49) Stratmann, R. E.; Scuseria, G.; Frisch, M. J. *J. Chem. Phys.* **1998**, *109*, 8218.
 (50) Görling, A.; Heinze, H. H.; Ruzankin, S. P.; Stauffer, M.; Rösch, N. *J. Chem. Phys.* **1999**, *110*, 2785.
 (51) Raghavachari, K.; Ricci, D.; Pacchioni, G. *J. Chem. Phys.* **2002**, *116*, 825.

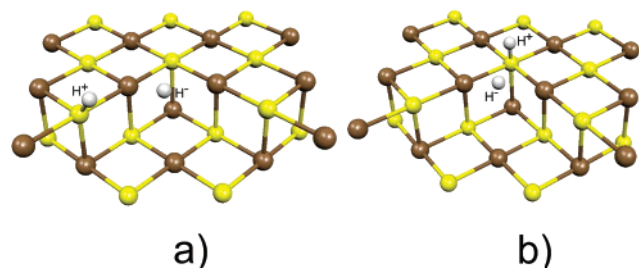


Figure 3. Optimal structure of a H_2 molecule dissociatively adsorbed on a MgO_{RC} site, $\text{MgO}(\text{H}^+)(\text{H}^-)$. (a) Configuration 1 with the proton adsorbed on a step $\text{O}_{4\text{c}}$ site; (b) configuration 2 with the proton adsorbed on a $\text{O}_{5\text{c}}$ site at the reverse corner site. Dark spheres, Mg; white spheres, O.

of adsorption measured with an accurate calorimetric apparatus is about 0.5 eV.⁵²

The next question which has to be answered is whether the described above dissociative adsorption of H_2 is an activated process. This is quite relevant because experimentally it has been observed that H_2 dissociation takes place at low temperature, suggesting the existence of a very small barrier or of a nonactivated process. We have first performed a search for the transition state (TS) using the Berny algorithm.⁵³ The calculations have been done for configuration 1 with the standard Gaussian 98 code and with a smaller cluster, $\text{Mg}_{10}\text{O}_{10}$, embedded in point charges and ECPs to (i) exploit the possibility to perform a search for a TS not yet implemented in the GUESS code and (ii) reduce the cost of the calculations. With this cluster, the H_2 dissociation is exothermic by 0.8 eV (instead of 0.5 eV as obtained with the larger cluster and the shell model embedding), but the geometry is close to that of the previous one. However, the qualitative conclusions about the shape of the potential energy surface should not change. All of the attempts to locate the TS failed, leading to gas-phase H_2 and MgO . This is strongly indicative of a nonactivated process. We have also performed a constraint optimization where only the H–H distance has been fixed (the values have been varied from 0.74 to 2 Å), and all of the rest of the system has been reoptimized. In this way, we have obtained a section of the potential energy surface along the most important internal coordinate, the H–H distance. The results, Figure 4, show that the H_2 molecule is dissociatively adsorbed with a barrier of less than 0.05 eV. This barrier, however, is due to the constraint optimization and disappears when a full TS search is performed. This is an important result which shows that the associative desorption of H_2 implies a cost of +0.54 eV (shell model result), an energy which suggests that the adsorbed $(\text{H}^+)(\text{H}^-)$ complex will not survive above room temperature.

C. Vibrational Properties of the $\text{MgO}_{\text{RC}}(\text{H}^+)(\text{H}^-)$ Complex. Here we compare the calculated vibrational frequencies of the $\text{MgO}_{\text{RC}}(\text{H}^+)(\text{H}^-)$ complex with the those of the experimental data. Experimentally, it has been established that there are two forms of dissociatively adsorbed H_2 present on the MgO surface: one irreversibly adsorbed and stable up to 400 K,^{54,55} and another one reversibly adsorbed, which is removed by

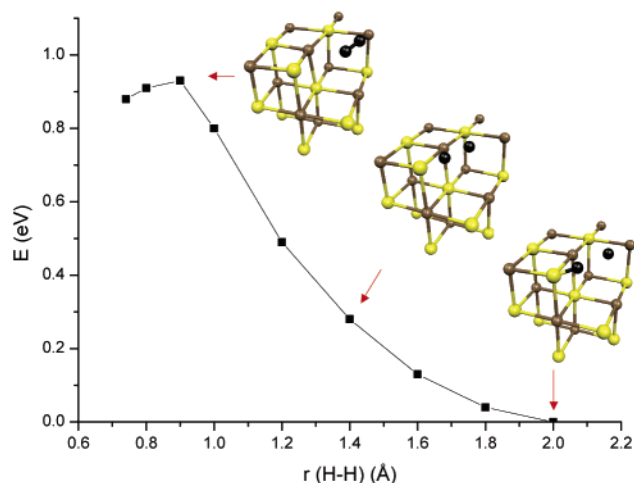


Figure 4. Section of the potential energy surface for the interaction of H_2 with a $\text{Mg}_{10}\text{O}_{10}$ cluster model of a reverse corner site, MgO_{RC} . For each fixed H–H distance, the rest of the geometrical parameters have been reoptimized. The position of the H atoms (black spheres) for three structures is shown.

Table 1. Experimental and Calculated Vibrational Stretching Frequencies of O–H and Mg–H Groups on the Surface of MgO

	exp. [10, 56–59]		theory	
	$\nu(\text{O–H})$, cm^{-1}	$\nu(\text{Mg–H})$, cm^{-1}	$\nu(\text{O–H})$, cm^{-1}	$\nu(\text{Mg–H})$, cm^{-1}
irreversibly adsorbed H_2	3712	1130	3730	1039
reversibly adsorbed H_2	3462	1325	3765	1227
after UV irradiation	3632, 3602, 3528		3472	
			$\text{MgO}_{\text{RC}}(\text{H}^+)(\text{H}^-)$	$\text{MgO}_{\text{RC}}(\text{H}^+)(\text{H}^-)$
			$\text{MgO}_{\text{RC}}(\text{H}^+)(\text{e}^-)$	$\text{MgO}_{\text{RC}}(\text{H}^+)(\text{e}^-)$
			$\text{MgO}_{\text{step}}(\text{H}^+)(\text{e}^-)$	

evacuation of the H_2 gas at 300 K.^{10,28,56–59} Irreversible H_2 gives rise to two well identified frequencies, at 3712 and at 1130 cm^{-1} ; the reversibly adsorbed H_2 shows two bands which are red- and blue-shifted, respectively, with respect to those of the irreversible form: 3462 and 1325 cm^{-1} , Table 1.^{10,56,57} The bands at 3500–3700 cm^{-1} have been assigned to OH groups, and those at 1100–1300 cm^{-1} have been assigned to hydride species, respectively. The shifts in the two bands represent a fingerprint of the two kinds of adsorbed hydrogen, reversible (3462 and 1325 cm^{-1}) and irreversible (3712 and 1130 cm^{-1}).

We have computed the vibrational frequencies for the $\text{MgO}_{\text{RC}}(\text{H}^+)(\text{H}^-)$ complex **1** as well as for isolated H^+ and H^- species independently adsorbed on the same MgO_{RC} site; a proton has been added to an edge atom to give $\text{MgO}_{\text{RC}}(\text{H}^+)$, and an H^- ion has been placed at the reverse corner site, $\text{MgO}_{\text{RC}}(\text{H}^-)$. The OH frequency in $\text{MgO}_{\text{RC}}(\text{H}^+)$, 3730 cm^{-1} , Table 1, is close to that measured for irreversibly adsorbed H_2 , 3712 cm^{-1} , and falls in the narrow range of frequencies (3746–3725 cm^{-1}) measured for isolated OH groups at the surface of MgO during the final stages of the progressive dehydration of

(52) Chiesa, M.; Giamello, E.; Paganini, M. C., to be published.

(53) Schlegel, H. B. In *Modern Electronic Structure Theory*; Yarkony, D. R., Ed.; World Scientific: Singapore, 1995.

(54) Ito, T.; Kuramoto, M.; Yoshioka, M.; Tokuda, T. *J. Phys. Chem.* **1983**, *87*, 4411.

(55) Ito, T.; Murakami, T.; Tokuda, T. *J. Chem. Soc., Faraday Trans. 1* **1983**, *79*, 913.

(56) Coluccia, S.; Boccuzzi, F.; Ghiotti, G.; Morterra C. *J. Chem. Soc., Faraday Trans.* **1982**, *78*, 2111.

(57) Diwald, O.; Hoffman, P.; Knoezinger, E. *Phys. Chem. Chem. Phys.* **1999**, *1*, 713.

(58) Diwald, O.; Knoezinger, E.; Martra, G. *J. Chem. Phys.* **1999**, *111*, 6668.

(59) Diwald, O.; Berger, T.; Sterrer, M.; Knoezinger, E. *Stud. Surf. Sci. Catal.* **2001**, *140*, 237.

the oxide.⁶⁰ The isolated $\text{MgO}_{\text{RC}}(\text{H}^-)$ gives rise to two stretching frequencies at 1039 and 1023 cm^{-1} and a motion at 732 cm^{-1} . The frequencies at 1039 and 1023 cm^{-1} are somewhat smaller than the experimental hydride bands and, in particular, the band at 1130 cm^{-1} assigned to the irreversibly bound H^- . Let us consider now the $\text{MgO}_{\text{RC}}(\text{H}^+)(\text{H}^-)$ configuration 1. This exhibits an OH stretching at 3675 cm^{-1} , Table 1, 55 cm^{-1} smaller than that for the free OH group in the same location. The lower frequency of the OH stretching in $\text{MgO}_{\text{RC}}(\text{H}^+)(\text{H}^-)$ is due to the interaction with the nearby H^- ion, but the shift is much smaller than that observed experimentally, 250 cm^{-1} . The other frequencies of the $\text{MgO}_{\text{RC}}(\text{H}^+)(\text{H}^-)$ complex are at 1227 cm^{-1} (corresponding to a parallel motion of the H^- ion to the surface), at 895 cm^{-1} (OH bending), and at 661 and 534 cm^{-1} (mixed OH bending and H^- stretching). Thus, the vibration of H^- in $\text{MgO}_{\text{RC}}(\text{H}^+)(\text{H}^-)$ is blue-shifted by 200 cm^{-1} with respect to that calculated for the isolated $\text{MgO}_{\text{RC}}(\text{H}^-)$. This latter value nicely fits with the corresponding differences between the experimental values of reversible and irreversible hydrides, 195 cm^{-1} .

We can therefore advance the following working hypothesis. The two H^+-H^- pairs (“reversible” and “irreversible”) could have the same structure but different distance between the two fragments, the mutual interaction of the H^+ and H^- fragments being responsible for the frequency shifts observed for “reversibly” adsorbed H_2 . In the reversible complex, the $\text{H}-\text{H}$ distance is short, and the recombination of the two atoms to give H_2 is possible without implying a complex diffusion path on the surface; in the irreversible form, the two charged species are separated by a large distance so that the corresponding vibrational modes are pure, and the recombination is unlikely. The vibration at 534 cm^{-1} in the $\text{MgO}_{\text{RC}}(\text{H}^+)(\text{H}^-)$ has the special feature to bring the H^+ and H^- fragments closer together and represents the natural channel for the recombination of the two atoms and the formation of the H_2 molecule as the temperature is raised.

Thus, both the energy data and the vibrational analysis suggest that the species investigated here correspond to reversibly adsorbed H_2 . This conclusion is based on four different observations: (i) the energetics of the reaction, exothermic by about 0.5 eV, is consistent with the calorimetric measurements; (ii) the occurrence of the reaction at low temperature, 77 K, is consistent with a nonactivated process; (iii) the vibrational frequencies are shifted with respect to those of the isolated H^+ and H^- adsorbates, consistent with the shift of the bands observed for the reversible form of H_2 ; and (iv) on the $\text{MgO}_{\text{RC}}(\text{H}^+)(\text{H}^-)$ complex, there is one vibrational mode at 534 cm^{-1} which brings the H^+ and H^- fragments closer together and which is responsible for the recombinative process as the temperature increases.

D. Structure of $\text{MgO}(\text{H}^+)(\text{e}^-)_{\text{trapped}}$ Defect Centers. In the previous section, we have shown that a MgO_{RC} site is able to reversibly adsorb and dissociate H_2 at low temperature. The resulting $\text{MgO}_{\text{RC}}(\text{H}^+)(\text{H}^-)$ center is diamagnetic, and in fact no increase of the EPR signal is observed in these conditions. However, if the sample is exposed to UV irradiation, one observes a change in the color of the sample which is accompanied by a concomitant increase of the typical EPR

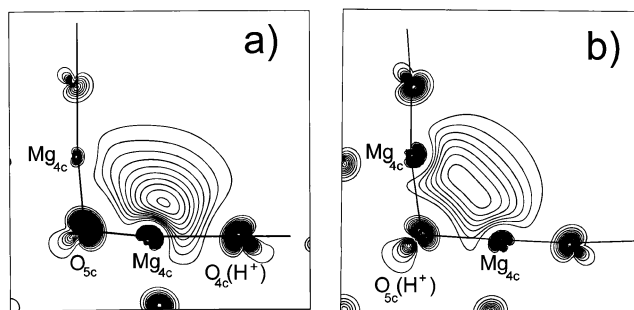


Figure 5. Spin density map of the $\text{MgO}_{\text{RC}}(\text{H}^+)(\text{e}^-)_{\text{trapped}}$ center plotted in the plane of the surface layer. (a) Configuration 1 with the proton adsorbed on a step $\text{O}_{4\text{c}}$ site; (b) configuration 2 with the proton adsorbed on a $\text{O}_{5\text{c}}$ site at the reverse corner site.

signal of an $\text{F}_5(\text{H}^+)$ center.⁹ Our calculations show that the energy required to desorb a neutral H atom from the $\text{MgO}_{\text{RC}}(\text{H}^+)(\text{H}^-)$ center, reaction 2, is 3.56 eV for configuration 1 and 3.65 eV for configuration 2. This corresponds to the near-UV region and could explain why UV irradiation is required to form the $\text{F}_5(\text{H}^+)$ center. However, the detailed mechanism of reaction 2 requires a more thorough study.

If one atom is removed from the system, the remaining $\text{MgO}_{\text{RC}}(\text{H}^+)(\text{e}^-)_{\text{trapped}}$ center corresponds to an electron stabilized by an adsorbed proton. This is clearly shown by the spin density maps in Figure 5, which indicate that the electron is trapped at the site defined by the three Mg^{2+} cations of the reverse corner considered with the proton adsorbed either on $\text{O}_{4\text{c}}$ or on $\text{O}_{5\text{c}}$ (configurations 1 and 2 in Figure 3a and b, respectively). Not to increase the number of notations, in the following discussion, we will continue using notations “configuration 1” and “configuration 2” also for the two configurations of the $\text{MgO}_{\text{RC}}(\text{H}^+)(\text{e}^-)_{\text{trapped}}$ center shown in Figure 5a and b. Configuration 1 is more favorable than configuration 2 by 0.40 eV. The fact that the H atom adsorbed at the MgO_{RC} site spontaneously evolves toward $(\text{H}^+) + (\text{e}^-)_{\text{trapped}}$ agrees with the experimental observation of $\text{F}_5(\text{H}^+)$ centers after treating the MgO powder with atomic hydrogen,⁸ with the mechanism indicated in reaction 3.

E. Properties of the $\text{MgO}_{\text{RC}}(\text{H}^+)(\text{e}^-)_{\text{trapped}}$ Defect Centers. The result of reactions 2 and 3 is that one forms on the surface a deep trap for a single electron, $\text{MgO}_{\text{RC}}(\text{H}^+)(\text{e}^-)_{\text{trapped}}$. The resulting defect center has specific properties, which can allow one to identify and characterize it both experimentally and theoretically. In particular, the vertical EA of the $\text{MgO}_{\text{RC}}(\text{H}^+)$ centers is 3.07 eV. The vertical IP of the $\text{MgO}_{\text{RC}}(\text{H}^+)(\text{e}^-)_{\text{trapped}}$ center, that is, the energy required to remove the electron after it has been bound to the site and the structure has been reoptimized, is even higher, 4.76 eV, showing that (a) the centers are stable at temperatures well above room temperature, and (b) they can, in principle, give rise to the specific optical absorption bands in the visible region, thus explaining the color of the sample. Another proof of the strong stabilizing action of the adsorbed proton is that the $\text{MgO}_{\text{RC}}(\text{H}^+)(\text{e}^-)_{\text{trapped}}$ center has a positive vertical EA of about 1.0 eV. This means that this center can, in principle, trap another electron and transform into a site where two electrons are bound. The resulting diamagnetic defect center is negatively charged (one proton and two electrons) and is reminiscent of the classical neutral F_5 center model of an oxygen vacancy, with two associated electrons. The ability of $\text{MgO}_{\text{RC}}(\text{H}^+)(\text{e}^-)_{\text{trapped}}$ to bind a second electron

(60) Coluccia, S.; Lavagnino, S.; Marchese, L. *Mater. Chem. Phys.* **1988**, *18*, 445.

Table 2. Experimental and Calculated Hyperfine Coupling Constants of Paramagnetic Centers at the Surface of MgO

	$a_{\text{iso}}(^{25}\text{Mg}_{4c}), \text{G}$	$a_{\text{iso}}(^{25}\text{Mg}_{5c}), \text{G}$	$a_{\text{iso}}(^1\text{H}), \text{G}$
Mg _{ORC} (H ⁺)(e ⁻) 1	26.9	0.8	3.1
Mg _{ORC} (H ⁺)(e ⁻) 2	15.2	0.8	3.6
Mg _{Ostep} (H ⁺)(e ⁻) asym	34.2	1.1	4.4
Mg _{Ostep} (H ⁺)(e ⁻) sym	13.7, 12.2	1.1	4.2
F _S (H ⁺) exp. [9]	10.5	0.7	2.1

requires, however, further theoretical investigations and experimental evidence.

Yet another powerful method for identifying these centers is vibrational spectroscopy. In particular, the vibration of the OH group is influenced by the presence of the trapped electron; the computed O–H stretching in Mg_{ORC}(H⁺)(e⁻)_{trapped}, 3474 cm⁻¹, is 256 cm⁻¹ smaller than that computed for the Mg_{ORC}(H⁺) system, Table 1. A dramatic change in the OH frequencies has been monitored by Knözinger and co-workers,^{57–59} who found that upon UV irradiation and (H⁺)–(e⁻) formation new IR bands are found at 3528, 3602, and 3632 cm⁻¹, Table 1, with redshifts of up to 180 cm⁻¹ with respect to isolated OH groups.

Detailed characterization of the F_S(H)⁺ center is provided by the EPR technique. The EPR measurements⁹ attributed to the F_S(H)⁺ centers suggest that (a) the unpaired electron interacts with an H atom which should be a few Å apart (¹H hyperfine splitting of 2.1 G for the perpendicular component of the tensor), (b) the electron interacts with more than just one Mg ion, and (c) the spin density is inhomogeneous: in fact, two hyperfine isotropic coupling constants with the ²⁵Mg nuclide have been measured, 10.5 and 0.7 G, respectively, Table 2.

In the case of Mg_{ORC}(H⁺)(e⁻)_{trapped} in configuration 1, the trapped electron interacts preferentially with the Mg_{4c} cation which is nearest to the OH group, Figure 5a; the resulting a_{iso} , 26.9 G, is much larger than that observed experimentally.^{9,10} The a_{iso} for the other Mg_{4c} ion of the reverse corner is 2.8 G, while for the Mg_{5c} ion it is 0.8 G. The coupling with the H nucleus, 3.1 G, is reasonably close to the measured one, Table 2. In configuration 2, Figure 5b, the proton is in a symmetric position with respect to the two Mg_{4c} ions, and a_{iso} for the two equivalent ²⁵Mg nuclides is 15.2 G; that for the basal Mg_{5c} ion is 0.8 G, and that for H is 3.6 G, Table 2. The overall agreement with the experimental data is better, but configuration 2 is about 0.4 eV less stable than configuration 1. Thus, the Mg_{ORC}(H⁺)(e⁻)_{trapped} model of an F_S(H)⁺ center is consistent with the EPR spectra only if one assumes that the proton is in a symmetric position, although the calculations do not indicate this as the most favored structure. A symmetric case with an H atom adsorbed at the step is further considered in section 3f.

Another aspect which needs to be verified is the electronic transitions of the trapped electron in MgO(H⁺)(e⁻)_{trapped}. These transitions are responsible for the color of the sample. Starting from the doublet ground state of Mg_{ORC}(H⁺)(e⁻)_{trapped}, the transition energies have been computed within TD-DFT. The lowest doublet-to-doublet excitation is a HOMO–LUMO transition which occurs at 1.98 eV and has the transition matrix element of 0.2; this is followed by other less intense transitions from 2.5 to 3 eV which however involve more delocalized states near or in the conduction band. A transition of about 2 eV is quite consistent with experimental measurements on both single

crystal⁶¹ and thin film⁶² MgO samples which show optical transitions at 2–2.5 eV. It should be noted, however, that (a) the accuracy of TD-DFT for this kind of transitions has still to be proved and (b) the above experiments performed on single crystals or thin films refer probably to different defects, like oxygen vacancies, and not to the F_S(H)⁺ centers described here.

On the other hand, diffuse reflectance UV–vis experiments on polycrystalline MgO where F_S(H)⁺ defect centers have been created according to reactions 1 and 2 exhibit an absorption band at 520 nm (2.4 eV),¹⁰ which would be quite consistent with the optical transition at 2 eV predicted by TD-DFT for the Mg_{ORC}(H⁺)(e⁻)_{trapped} center. The important conclusion here is that an electron trapped at a reverse corner site in the proximity of a proton gives rise to electronic transitions which are comparable to those of the classical surface F centers.

F. MgO(H⁺)(e⁻)_{trapped} Defect Centers at Steps. The results presented above give an example of a consistent approach to building a model of the F_S(H)⁺ center at the MgO(001) surface based solely on reactions 1–3 and on the surface morphology. It is clear that there is a variety of low-coordinated sites at real surfaces, and we believe that many of them can give rise to the H₂ dissociation (see also refs 63 and 64) and formation of F_S(H⁺)-like centers. To make this point stronger, we demonstrate in this section that the above discussion is valid also for H₂ interaction with MgO steps consisting of four-coordinated Mg and O ions.

Previous cluster calculations^{65,66} have shown the tendency of low-coordinated Mg_{3c} and O_{3c} ions at corner sites to easily dissociate heterolytically the H₂ molecule, while it is not entirely clear if such dissociation can occur at four-coordinated edge sites. To the best of our knowledge, however, the step site has never been investigated before. Our calculations demonstrate that the Mg_{Ostep}(H⁺)(H⁻) complex with H⁺ and H⁻ being at the neighboring four-coordinated sites is by 0.6 eV more stable than free H₂ molecule and MgO step. We did not model the dissociation mechanism of the H₂ molecule, but rather we focused on the properties of an H atom adsorbed at the step edge. Although they can be expected to be similar to those of the configuration 1 of the Mg_{ORC}(H⁺)(e⁻) center considered above, the step center is more symmetric, and this study can shed some further light on the EPR properties of proton-stabilized electron centers.

Our calculations demonstrate that one can distinguish at least two configurations of H atom adsorbed at the step: (i) a symmetric configuration in which the OH bond is fixed in the direction perpendicular to the step line, Figure 6a, and (ii) an asymmetric (tilted) configuration in which the H atom is tilted to one of the two nearby Mg ions, Figure 6b. We find that the asymmetric configuration is more stable by 0.19 eV; that is, the symmetric configuration represents a transition state between the two equivalent asymmetric configurations. In both cases, the H atom dissociates into H⁺ and e⁻ with formation of an Mg_{Ostep}(H⁺)(e⁻)_{trapped} center with the electron localized on a

- (61) Henrich, V. E.; Dresselhaus, G.; Zeiger, H. *J. Phys. Rev. B* **1980**, *22*, 4764.
 (62) Peterka, D. C.; Tegenkamp, K.; Schröder, M.; Ernst, W.; Pfnür, H. *Surf. Sci.* **1999**, *431*, 146.
 (63) Ito, T.; Kuramoto, M.; Yoshioka, M.; Tokuda, T. *J. Phys. Chem.* **1983**, *87*, 4411.
 (64) Ito, T.; Murakami, T.; Tokuda, T. *J. Chem. Soc., Faraday Trans. 1* **1983**, *79*, 913.
 (65) Sawabe, K.; Koga, N.; Morokuma, K.; Iwasawa, Y. *J. Chem. Phys.* **1994**, *101*, 4819.
 (66) Kobayashi, H.; Salahub, D. R.; Ito, T. *J. Phys. Chem.* **1994**, *98*, 5487.

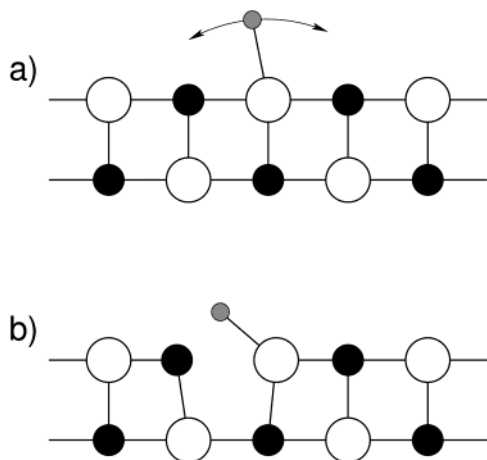


Figure 6. Schematic representation of a proton adsorbed on a step site of the MgO surface. (a) Symmetric configuration (vibration of the proton around its symmetrical position is shown); (b) asymmetric configuration.

single Mg ion in the tilted configuration and delocalized over two Mg ions in the symmetric one. In the case of the tilted configuration, the trapped electron interacts strongly with one Mg ion, which results in the calculated a_{iso} of 34.2 G, Table 2. This is close to the value found for the configuration 1 above and more than 3 times larger than the experimentally observed a_{iso} for the $\text{F}_S(\text{H})^+$ center.⁹ In the case of symmetric configuration, the trapped electron is more delocalized, and the calculated a_{iso} 's with the two Mg_{4c} ions are 13.7 and 12.2 G, Table 2 (the difference appears due to the spontaneous break of the local symmetry). Other a_{iso} constants are 1.1 G for the Mg_{5c} in the upper terrace of the step and 0.8 and 0.7 G for two Mg_{5c} in the lower terrace. The coupling with the H nucleus is about 4.2 G, Table 2. Again we observe that the hyperfine constants calculated for the symmetric configuration are in better agreement with the experimental data.⁹

To characterize the $\text{MgO}_{\text{step}}(\text{H}^+)(e^-)_{\text{trapped}}$ further, we calculated the vertical IPs for both configurations. The resulting values, 3.17 eV for the symmetric configuration and 3.71 eV for the asymmetric one, suggest that, similar to the $\text{MgO}_{\text{RC}}(\text{H}^+)(e^-)_{\text{trapped}}$, these centers are stable at room temperature and may give rise to an optical absorption in the visible part of the UV spectrum. The lowest doublet-to-doublet excitation energies calculated for the symmetric configuration using the TD-DFT approach are 1.29 and 2.12 eV with the transition matrix elements of 0.24 and 0.16, respectively. Excitation energies for the asymmetric configuration are 1.79 and 2.42 eV with transition matrix elements of 0.12 and 0.14, respectively.

Finally, we wish to comment on the dynamics of the $\text{MgO}_{\text{step}}(\text{H}^+)(e^-)_{\text{trapped}}$ center. We note that (i) the proton is very light as compared to the MgO lattice ions and (ii) the calculated barrier for the proton flipping between two asymmetric configurations is only 0.2 eV. We, therefore, suggest that the proton flips between the two tilted configurations so fast that the lattice cannot follow its motion. Instead, the lattice ions fluctuate near their positions, which correspond to the average configuration of the OH bond, that is, the symmetric configuration. In this case, the potential energy surface (PES) for the OH bending has a single rather than double well profile.

To clarify this issue, we have calculated vibrational frequencies for the H atom motion in the more stable asymmetric configuration. The vibration, which corresponds to motion

between the two asymmetric configurations, has a frequency of 786 cm^{-1} . Therefore, the zero point energy level for the proton motion along the step is only about 0.1 eV below the energy of the symmetrical configuration, which is the barrier state for such motion. This further supports the suggestion that at finite temperatures, the proton moves in the single rather than double well potential. Recent experiments on the temperature dependence of the hyperfine interaction of the $\text{F}_S(\text{H})^+$ center found a slight decrease of the $a_{\text{iso}}(^{25}\text{Mg})$ with the temperature change from 77 to 4 K.⁶⁷ This result is consistent with the motion of the proton in the single well PES and rules out the conversion of the $\text{MgO}_{\text{step}}(\text{H}^+)(e^-)_{\text{trapped}}$ center from the symmetric to the asymmetric configuration at low temperatures.

To summarize, the considered properties of the $\text{MgO}_{\text{step}}(\text{H}^+)(e^-)_{\text{trapped}}$ are very similar to those of the $\text{MgO}_{\text{RC}}(\text{H}^+)(e^-)_{\text{trapped}}$ center. Together, MgO_{step} and MgO_{RC} are likely to be representatives of a larger class of surface defect sites, which give rise to a number of paramagnetic centers consistent with those of the observed $\text{F}_S(\text{H})^+$ complex.

G. Adsorption of H Atoms at $\text{MgO}(001)$ Terrace. The results presented in previous sections demonstrate that hydrogen atom adsorbed at reverse corner or step tends to form a center which can be characterized as an electron at the Mg site stabilized by the proton adsorbed on the nearby oxygen ion. It is interesting to see whether this is a general effect, which will take place also at, for example, ideal surface terrace. The DFT calculations in the same setup as those described above show, however, that an H atom on-top of an O_{5c} ion on the $\text{MgO}(001)$ terrace is weakly bound by about 0.5 eV and that the unpaired electron resides largely on the hydrogen. This could result from the well-known tendency of DFT to delocalize trapped electron and hole states (see, for example, ref 68). Therefore, we carried out the Hartree–Fock (HF) calculations for this system too. These calculations give the H atom adsorption energy close to zero and the distribution of the electronic charge similar to that obtained in DFT calculations, that is, no electron transfer to Mg ions. These results demonstrate that the hydrogen atom is indeed weakly bound and suggest that it can be very mobile at a terrace.

The remarkable difference in the mode of adsorption of the H atom at the terrace and steps and corner sites can be understood if we consider the main factors which determine the adsorption mechanism. The high cost for H ionization is compensated by at least four energy contributions. The first one is the proton affinity of a surface O^{2-} ion, which is close to 12 eV, the second is that a reverse corner at the MgO surface is a shallow electron trap with an EA of about 1 eV (see section 3a), the third one is the electrostatic interaction of a positively charged proton and the trapped electron, and finally the fourth one is due to the lattice relaxation around the electron trapped on Mg ions. The very small, if any, electron affinity combined with a much tougher lattice surrounding the Mg site on a terrace¹³ tips the balance toward the H atom rather than the electron stabilized by proton configuration.

4. Conclusions

The real nature of paramagnetic defect centers at the MgO surface has been the matter of debate in recent years. Because

(67) Chiesa, M.; Giamello, E., to be published.

(68) Pacchioni, G.; Frigoli, F.; Ricci, D.; Weil, J. A. *Phys. Rev. B* **2001**, *63*, 054102.

these centers play a crucial role in the surface chemistry of MgO and other ionic oxides, a detailed knowledge of their structure is essential to rationalize a number of features associated with their presence.

In this paper, we have addressed specifically the nature of what is usually called the $F_S(H)^+$ center, an electron trapped in the vicinity of an adsorbed proton. This center can be chemically generated by H_2 adsorption followed by UV irradiation and gives rise to a characteristic and well reproducible EPR signal.¹⁰ In particular, we have considered two surface sites, the reverse corner, MgO_{RC} , and the step, MgO_{step} , which do not belong to the class of “oxygen vacancies” used so far to explain the formation of paramagnetic color centers. According to this proposal, these sites are the precursors of the $MgO_{RC}(H^+)(e^-)_{trapped}$ and $MgO_{step}(H^+)(e^-)_{trapped}$ centers, which are the actual structures of two of the many possible surface $F_S(H)^+$ paramagnetic defect centers. The presence at the surface, in fact, of more than one type of distinct $F_S(H)^+$ has been inferred by simulation of the EPR signal,⁹ by direct ENDOR observation of two centers with different hyperfine coupling constant,²⁹ and by the observation of a variety of O^- centers formed by bleaching the surface containing $F_S(H)^+$ with N_2O .³⁰ The two sites discussed above were never proposed before as possible electron traps and can be considered as the prototypes of a new family of surface traps. They represent “natural” morphological features abundant at real surfaces and not requiring the high formation energy of other traps such as the widely analyzed oxygen vacancies. The MgO_{RC} center considered in more detail in this paper fits a number of observations:

(1) The MgO_{RC} site dissociates the H_2 molecule with a nonactivated exothermic reaction; the computed energy release, 0.5 eV, is surprisingly close to that measured by calorimetric experiments.⁵²

(2) The structure of the resulting $MgO_{RC}(H^+)(H^-)$ center is consistent with a heterolytic dissociation of H_2 ; the formation of (H^+) and (H^-) fragments is shown by the very different vibrational spectra of the two species. In particular, the vibrational analysis for $MgO_{RC}(H^+)(H^-)$ strongly suggests that this is the surface complex resulting from reversibly adsorbed H_2 . The irreversible form of adsorbed H_2 observed experimentally probably consists of similar (H^+) and (H^-) fragments separated by long distances.

(3) The removal of a neutral H atom from the diamagnetic $MgO_{RC}(H^+)(H^-)$ center has a cost of about 3.5 eV, consistent with the use of UV light for the process, and results in a trapped electron at the MgO surface, $MgO_{RC}(H^+)(e^-)_{trapped}$. In this structure, the electron is localized in the site formed by the conjunction of two steps and gives rise to a typical EPR signal. The removal of this electron costs more than 4 eV, so not only the center is thermally stable, but also electronic excitations in the visible region are possible, justifying the coloring of the sample connected to the presence of these centers.

(4) The analysis of the isotropic hyperfine coupling constants provides support to the proposed model assuming that the adsorbed proton lies in a symmetric position between two four-coordinated Mg cations.

(5) The computed lowest transition for the trapped electron, about 2 eV, is close to values reported for optical excitations at the surface of polycrystalline MgO where $F_S(H)^+$ defect centers have been created according to reactions 1–3.

Table 3. Dependence of the Electron Affinity, EA in eV, for the MgO_{RC} Site on Cluster Stoichiometry and Treatment of Interface Mg^+ Atoms^a

cluster	Mg^+ (ECP) ^b		Mg^+ (AE) ^b	
	CEP	LANL1	minimal basis	split basis
$Mg_{23}O_{17}Mg^{*16}$	1.59	1.62	1.98	1.98
$Mg_{21}O_{17}Mg^{*18}$	1.49	1.53	1.93	1.93
$Mg_{19}O_{17}Mg^{*20}$	1.33	1.38	1.85	1.85
$Mg_{17}O_{17}Mg^{*22}$	1.20	1.27	1.77	1.77
$Mg_{15}O_{17}Mg^{*24}$	0.82	0.89	1.55	1.55
$Mg_{13}O_{17}Mg^{*26}$	0.84	0.71	1.41	1.41
$Mg_{10}O_{17}Mg^{*29}$	0.35	0.43	1.18	1.18

^a Results obtained for truncated bulk geometries without including long-range polarization effects. ^b ECP = effective core potential; AE = all electron.

(6) Finally, we have shown that a reverse corner can also act as a shallow trap on the surface, with the ability to bind one electron and transform it into a paramagnetic center, $MgO_{RC}(e^-)_{trapped}$. The binding energy of the electron is comparable to that found for other shallow traps, in particular, divacancies or low-coordinated cations.

The results presented for a step further support the idea that a symmetric configuration of $MgO(H^+)(e^-)_{trapped}$ type defect can be responsible for the EPR signal attributed to $F_S(H)^+$ defect centers. Finally, we would like to note that similar centers can be formed by, for example, alkali and other adsorbed atoms, which can donate electrons to the surface and stabilize them by the Coulomb field. This may explain the formation of electronic centers at surfaces of other oxides.

Acknowledgment. This work has been supported by the “Italian INFN” through the PRA project ISADORA. P.V.S. and A.L.S. are grateful to PNNL for financial support. Pacific Northwest National Laboratory is operated for the U.S. Department of Energy by Battelle under Contract No. DE-AC06-76RLO 1830.

Appendix. Factors Affecting the Accuracy of Calculations

The results presented in section 3a predict positive electron affinities (EAs) for a reverse corner site which behaves in a way similar to that of other neutral shallow traps at the MgO surface. However, affinities on the order of 0.5–1 eV can be strongly affected by various computational factors. To assess the robustness of our qualitative predictions, we have analyzed in detail the effect of the interface atoms and of the cluster stoichiometry on the computed EAs, Table 3. The calculations have been done using various approaches to treat the interface atoms, Mg^* . These have been represented using either effective core potentials (ECP), in particular, the CEP³⁵ and LANL1⁶⁹ ECPs, or all electron (AE) Mg^{2+} ions using a limited basis set aimed to describe core ($1s^22s^22p^6$) states only. In this case too, we have considered two kinds of basis sets: both are derived from the Mg 6-31G basis by removing the external s and p functions. This leaves a minimal basis for the core (AE minimal basis); in a second case, the 1s, 2s, and 2p orbitals have been split to account for possible core polarization (AE split basis).

Clusters of various size have been used. They all have the same number of O atoms, 17, while the 39 Mg ions have been treated either as real QM ions or as interface Mg^* ions. $Mg_{10}O_{17}$ –

(69) Hay, P. J.; Wadt, W. R. *J. Chem. Phys.* **1985**, *82*, 270.

Mg*₂₉ has the smallest number of real and the largest number of interface Mg atoms; Mg₂₃O₁₇Mg*₁₆ has the opposite ratio. All of the clusters used, except Mg₁₇O₁₇Mg*₂₂ which has been adopted for the calculations reported in the paper, are nonstoichiometric so that the formal charge of the QM cluster has to be adjusted to take into account the formal +2 and -2 nature of the Mg and O ions in MgO, respectively. All of the calculations have been performed with Gaussian 98³⁷ at the B3LYP level for the geometry of the truncated bulk; thus, neither geometrical relaxation nor ion polarization is included.

We start by considering the effect of using CEP or LANL1 ECPs on the interface Mg* atoms, Table 3. The CEP ECP results in EAs which are smaller than those obtained with LANL1, but the differences are a few hundreds of an electronvolt. Things change dramatically when AE ions are used instead of ECPs. In fact, this results in a strong increase of the cluster EA. The largest variations are encountered for the MgO clusters with a smaller number of real cations (up to a 0.8 eV increase in EA); on the contrary, the changes for clusters with an excess of real cations are smaller (up to 0.4 eV). Notice that the use of a split basis set on the AE Mg* embedding atoms has no effect on the EAs, showing that the addition of an extra electron to the cluster does not result in a core polarization of the Mg ions.

The fact that the ECPs give consistently too small EAs suggests that they produce a too strong Coulomb repulsion with the neighboring O ions in the cluster anion. The electron added to the Mg_{ORC} site is mostly localized on the surface, Figure 2b; however, tails of the electron density are delocalized over the entire cluster, leading to an expansion of the O²⁻ anions: if the core region of the interface Mg* ions is too large, it results in a compression of the O²⁻ ions that destabilizes the system and leads to a reduction of EA. The ECPs used here to represent the core of the Mg²⁺ ions are obtained indeed on the neutral Mg atom. The [Ar] core of a neutral Mg atom is larger than that of a Mg²⁺ cation. In this respect, an AE treatment is likely to better represent the real size of the [Ar] core in Mg²⁺.

To confirm the validity of the above analysis, we have studied the 1s core level shifts of a bulk O²⁻ ion in MgO as described by a OMg₆ cluster embedded in shell models and classical ions. As a measure of the core level binding energy (BE), we take the reverse of the corresponding Kohn-Sahn eigenvalue. The use of CEP and LANL1 interface Mg* atoms gives an O 1s BE of 514.7 and 515.0 eV, respectively. In line with the EA results, the LANL1 ECP is more contracted and the electron cloud of the O²⁻ ion is slightly more expanded, thus reducing the Coulomb repulsion with a stabilization of 0.3 eV of the O 1s level as compared to the CEP ECP. The effect is much more pronounced with AE Mg* atoms: the O 1s BE is 517.3 eV (both with the minimal and with the split basis set); thus, the shift to higher BEs as compared to the ECP Mg* atoms is more than 2 eV. Because core level BEs are very sensitive to the local potential around the atom, these results provide a convincing proof of the important effect of the size of the core of the interface Mg* atoms. This effect, however, is largely restricted to the calculation of the EA of the site (cluster anion), while other properties of the neutral system are practically not affected by the choice of the interface embedding [see also ref 70].

A last comment is required on the performance of nonstoichiometric clusters. We have mentioned above that the largest dependence on the interface Mg* atoms is found for the clusters with an excess of embedding Mg* ions (e.g., Mg₁₀O₁₇Mg*₂₉, Table 3). The reason is clear if one considers the above discussion. Increasing the number of Mg ions which are replaced by ECPs reinforces the effect of compression on the O²⁻ ions. The opposite is true when an excess of real Mg atoms is present (see, e.g., Mg₂₃O₁₇Mg*₁₆). In this respect, the use of stoichiometric clusters is recommended.

JA0282240

(70) Yudanov, I. V.; Nasluzov, V. A.; Neyman, K. M.; Rösch, N. *Int. J. Quantum Chem.* **1997**, *65*, 975.